

# A thermostable trilayer resist for niobium lift-off

P. Dubos<sup>1</sup>, P. Charlat<sup>1</sup>, Th. Crozes<sup>1</sup>, P. Paniez<sup>2</sup> and B. Pannetier<sup>1</sup>

<sup>1</sup>*Centre de Recherches sur les Très Basses Températures, C.N.R.S.,  
Laboratoire conventionné avec l'Université Joseph Fourier,  
F-38042 Grenoble, France.*

<sup>2</sup>*France Telecom, C.N.E.T.- Grenoble, DTM/TFM, P.O. Box 98  
F-38243 Meylan Cedex, France*

We have developed a novel lift-off process for fabrication of high quality superconducting submicron niobium structures. The process makes use of a thermostable polymer with a high transition temperature  $T_g = 235^\circ\text{C}$  and an excellent chemical stability. The superconducting critical temperature of 100 nm wide niobium lines is above 7 K. An example of shadow evaporation of a Nb-Cu submicron hybrid structure is given. A potential application of this process is the fabrication of very small single electron devices using refractory metals.

PACS index category: 74.80 Fp, 85.25, 85.40

## I. INTRODUCTION

The field of single charge tunneling phenomena [1], mesoscopic superconductivity [2] or superconducting devices [3] has opened a new demand in high performance nanofabrication techniques with superior self-alignment capabilities. A common technique makes use of shadow evaporation through a suspended stencil mask prepared by electron beam lithography [4]. This technique allows self-alignment with nanometer scale accuracy as required for fabrication of ultrasmall tunnel junctions. Excellent results are currently obtained using conventional techniques based upon masks with PolyMethyl-MethAcrylate (PMMA) as the e-beam sensitive resist. The high resolution stencil mask is formed on top of a sub-layer with a well controlled undercut. The mask is easy to remove by a lift-off process. In the conventional two-layers process [5,6] the upper layer is a thin layer of PMMA (casting solvent Chlorobenzene) while the bottom layer is a copolymer PMMA-MAA containing MethAcrylic Acid (MAA) monomers. These MAA co-monomers make the copolymer soluble in polar solvents such as acetic acid and provide good chemical selectivity with respect to the top layer. Alternately the stencil mask can be made of a thin film of germanium or silicon patterned using an additionnal PMMA top layer (tri-layers process). Such a process, as well as more complex alternative processes with more than three layers, generally ensures excellent control of each intermediate step. It is widely used for the fabrication of devices made of soft materials such as aluminum, gold, copper, chromium, permalloy, etc. Structures of high complexity can be realized by multiple angle evaporation using one or two rotation axis [7].

Unfortunately, this technique cannot be extended to refractory metals such as niobium, molybdenum, tungsten or tantalum which require both high vacuum and high evaporation temperatures. As a consequence of the excessive heat produced by the electron beam evaporation, conventional resist masks are mechanically unstable. In addition, contamination due to the resulting outgasing of the resist degrades the electronic properties of the metal. It is a well known fact that the superconducting properties of niobium are extremely sensitive to a small amount of oxygen contamination [8]. Various methods have been attempted to extend the shadow evaporation technique to refractory metals with more stable mask structures. In Ref. [9], a combination of chromium mask with a metallic aluminum sub-layer was successfully used to fabricate arrays of micron size niobium/niobium Josephson junctions. More recently, Harada et al [10] developed a four layer resist system composed of PMMA, a hard baked photoresist, germanium and PMMA. This process was used successfully to fabricate submicron niobium/aluminum oxide/niobium superconducting single electron transistors. However, the measured critical temperature of the niobium electrode was far below that of the bulk material ( $9.2\text{K}$ ) and therefore the device could not reach optimum operation.

In this paper, we describe a new process based upon a thermostable polymer, the Poly PhenyleneEtherSulfone (PES) which greatly improves the quality of the devices. We present a detailed comparison between the thermal characteristics of this polysulfone and that of PMMA polymer. We show in particular why the latter should be avoided as a sub-layer resist. As a demonstrator for this process we have fabricated submicron niobium/copper/niobium Josephson junctions.

## II. SELECTION OF THE THERMOSTABLE BASE LAYER FOR THE TRILAYER PROCESS

We have chosen to develop a new trilayer process with a thermostable polymer as the base layer and silicon (alternately germanium) as the high resolution stencil mask. The thermal stability of the PMMA upper layer is irrelevant since this layer only serves for patterning the silicon mask and is removed before the evaporation process. In order to select an alternative to PMMA (or PMMA-MAA) as the bottom layer, we have explored a number of thermostable polymers of the phenolic family.

The first series of experiments was carried out on a PHS polymer (Poly ParaHydroxyStyrene) whose chemical formula is  $(CH_2 - CHX -)_n$  where X is the phenolic group. This polymer is a polystyrene with an hydroxyl function which insures solubility in polar solvents. Three different molecular weight have been used: 23.600, 30.000 and 109.000 g/mole. The powder was diluted in "Diglyme" (2-Methoxyethyl Ether). The glass transition temperature of this polymer is about 180°C. It can be safely used at temperatures below 240°C. Above this temperature, cross-linking makes the polymer insoluble. Good results were obtained with this polymer as a bottom layer in the trilayer process. However, it turned out to be damaged by the solvents used for the development and rinsing of the PMMA upper layer.

The best results were actually obtained with a polymer presenting a lower solubility: the poly PhenyleneEther-Sulfone (PES) originally commercially available under the name Victrex from ICI. This polymer is currently used as a thermostable organic substance for industrial use at 180°C. The chemical formula of PES is a sequence of aromatic groups attached to a sulfur atom. The monomer has the structure shown in Fig. 1a.

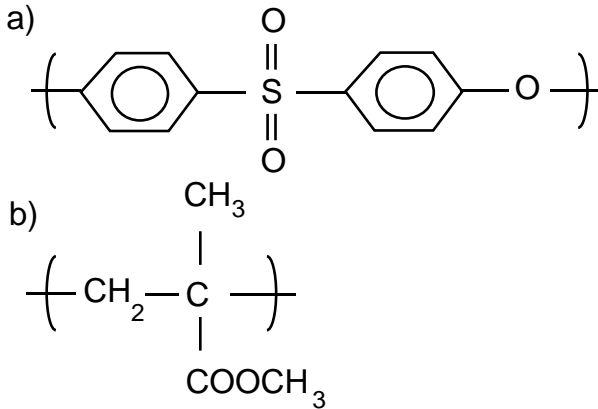


FIG. 1. a) The PES is a sequence of aromatic groups attached to a Sulfur atom. b) The PMMA chemical formula : the weak bond between monomers explains its high sensitivity to e-beam lithography and temperature.

The high thermal stability of PES is insured by the aromatic groups. We have used a Poly PhenyleneEtherSulfone with a high molecular weight: PES Victrex 5003P (ICI). The PES is dissolved in N-methyl Pyrrolidone (10% w/w) to form a solution that yields a standard thickness of a few hundred nanometers after spinning. For comparison the monomer of PMMA is described in Fig. 1b. The chemical bond between MMA monomers is weak. This is the reason for the excellent properties of PMMA as a high resolution and good sensitivity electron beam resist as well as its moderate thermal stability. The chemical properties of PES are also very attractive since this polymer exhibits a good compatibility with the organic solvents used in the subsequent steps of the trilayer process. It is inert in the PMMA solvents -

Chlorobenzene or Methyl-Iso-Butyl Ketone (MIBK) and is insoluble in IsoPropylic Alcohol. Its most convenient solvents are the DiMethyl Sulfoxide (DMSO) and the N-Methyl Pyrrolidone (NMP). The latter is much less dangerous and volatile than Chlorobenzene which is a standard solvent of PMMA.

### III. THERMAL CHARACTERISTICS OF THE BASE RESIST LAYER

The thermal properties of PMMA, PMMA-MAA and PES polymers were investigated using a TA Instruments 2950 Thermogravimetry Analyser (TGA) and a TA Instruments 2920 Differential Scanning Calorimetry (DSC) Analyser. The heating ramp for experiments was 10°C/min.

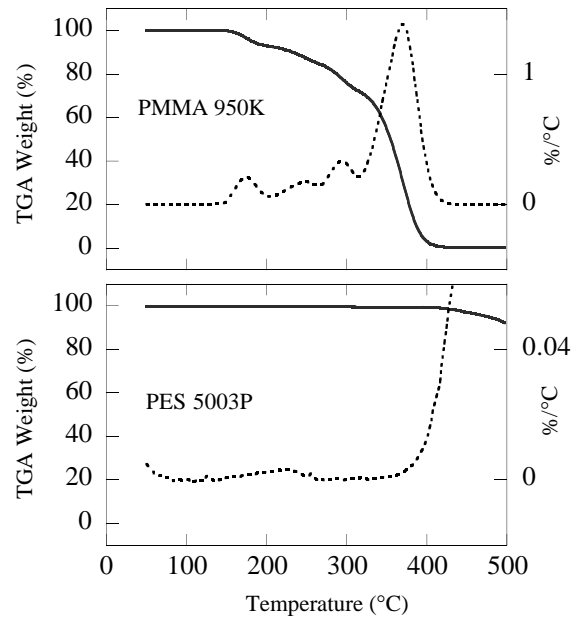


FIG. 2. Upper graph: TGA results for PMMA polymer with a molecular weight  $M_W = 950.000 \text{ g/mole}$ . Lower graph: TGA results for PES polysulfone. The full line indicates the weight loss vs. temperature in percent. The dashed lines represent the derivative of the TGA curves and indicate degassing of volatile species which are particularly abundant in PMMA.

The enhanced thermostability of PES is illustrated in Fig. 2 (lower graph) which demonstrates that its weight loss is negligible at temperatures up to 400°C, while a significant loss of weight is observed in PMMA at only 150°C. This temperature can easily be reached during e-beam evaporation of a refractory metal. The peaks in the derivative curve (dashed line) indicate the activation temperatures for chemical transformations such as anhydride formation or hydrocarbon outgassing which are important at moderate temperatures for PMMA. This polymer presents an extremely high chemical stabil-

ity between 275°C (hard-bake temperature) and 400°C. Above this temperature, the polymer properties degrade sharply.

Fig. 3 shows a Differential Scanning Calorimetry (DSC) thermogram of the two polymers. We found a glass transition temperature of respectively 235°C for PES and 121°C for PMMA, again showing the superior thermal properties of PES.

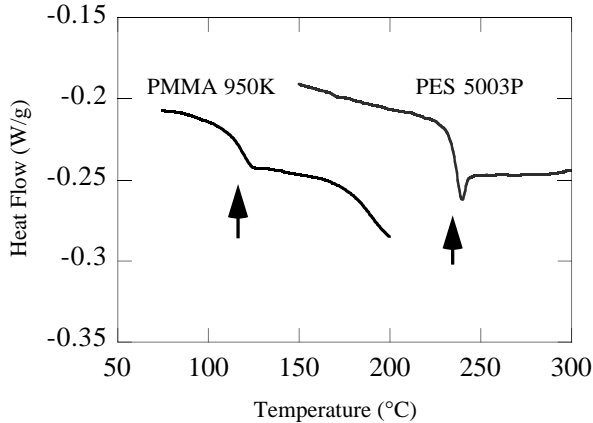


FIG. 3. Comparison of Differential Scanning Calorimetry (DSC) results for PES 5003P and PMMA 950K polymer. The arrows indicate the glass transition temperatures.

In general PMMA as well as its copolymers [11] are well known to exhibit poor thermal properties. In particular the PMMA-MAA copolymer exhibits low  $T_G$  (133°C for 8.5 % w/w of acid) and a high rate of weight loss at moderate temperatures [12]. As a result, a very strong outgassing of the resist bottom layer takes place in the vicinity of the device, even though no pressure increase was recorded by the vacuum gauge in our experiment. Indeed, we have observed that the niobium structures evaporated in a ultra-high vacuum chamber (base pressure of the chamber  $10^{-10}$  mbar, sample at 25 cm from niobium heated target) through a PMMA/PMMA-MAA bilayer, were not superconducting at 1K. We believe that the niobium film traps moisture, oxygen and hydrocarbons outgassed from the heated polymer sub-layer. We should mention that, with careful limitation of heat radiation eg. using copper shields, sequential evaporation and liquid nitrogen cooling of the substrate holder, intermediate superconducting critical temperatures could be achieved with a PMMA sub-layer. Additional improvement could even be obtained by encapsulating the PMMA resist with either silicon or aluminum oxide. As discussed below, the process based upon the PES thermostable sublayer is free of these constraints.

#### IV. PROCESS IMPLEMENTATION

The optimized trilayer fabrication process is as follows: Firstly, the PES 5003P solution (10% w/w in NMP) was spun on for 5 min at 2000 rpm on a 2 inch silicon wafer

to form the 300 nm thick bottom layer. After baking at 275°C for one minute on a hot-plate, a 40 nm thick silicon layer was e-beam evaporated at room temperature on the PES bottom layer. Alternately, germanium could be used without any change in the rest of the process. Finally a 85 nm thick PMMA layer (2% w/w PMMA 950K in chlorobenzene) was spun-on on top of the silicon. This thin PMMA layer was then patterned by electron beam lithography using a modified Scanning Electron Microscope Cambridge S240 with homemade interfaces for e-beam writing. Subsequently, the PMMA layer was developed in a solution (1:3) of MIBK and IsoPropyl Alcohol (IPA) for 20 seconds. The unprotected silicon was then removed by a Reactive Ion Etching (R.I.E.) in a Plassys MG200 reactor. The etching parameters were: 15 sec with 20 sccm  $SF_6$  at pressure  $2 \cdot 10^{-2}$  mbar, incident RF power 20 W, chamber at 15°C. We found it useful to place the substrate on a 4" pure silicon wafer in order to increase the etching time and optimize its reproducibility. Depending on the desired depth of undercut, two alternative processes could be used to etch the PES bottom layer [13]:

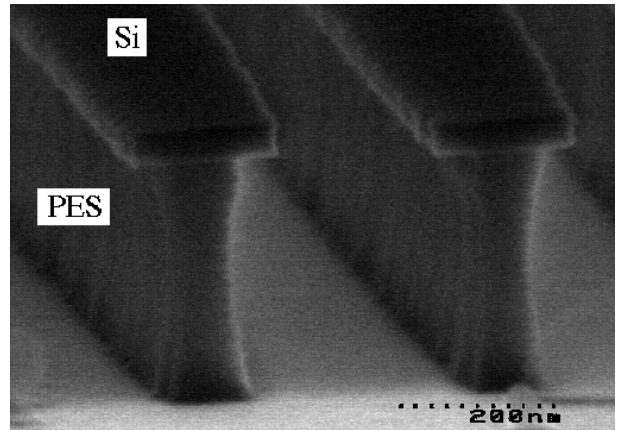


FIG. 4. Small undercut obtained by a dry process : R.I.E. oxygen for 3 min. The undercut is less than 50 nm. The walls of sub-layer PES resist are 320 nm high and 100 nm wide.

- small undercut : To obtain undercuts below 50 nm we used a dry process which consisted of an oxygen R.I.E. in the same reactor as above (but without the 4" pure silicon wafer). The etching conditions were the following : 3 min, 20 sccm oxygen at pressure  $4 \cdot 10^{-1}$  mbar, incident RF power 50W and chamber temperature at 15°C. An example of this dry process is shown in Fig. 4. This process can be extended to produce larger undercuts. However, residues of typical size 50 nm were usually obtained on the substrate. These residues are strongly resistant to R.I.E. and could only be eliminated using a wet process followed by additional oxygen plasma.

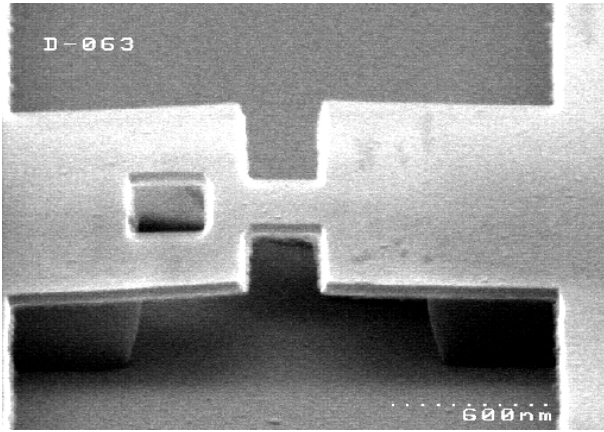


FIG. 5. Large undercut obtained in DMSO solvent. The PES resist is over-etched on 450 nm on both sides of a 300 nm wide hole in Silicon mask

- large undercut : To obtain undercuts larger than 50 nm a wet process based on DiMethyl Sulfoxide (DMSO) was found to be better. Thus, excellent control of both the etching time and temperature are extremely important since the etch rate is thermally activated. The sample was dipped and shaken into DMSO solvent kept at its melting temperature (18.6°C). We found that the undercut obeys a quasi-linear dependence as a function of etching time (see Table I) with a typical rate of 28 nm/sec. Ethanol was used both to stop the etching and to rinse the sample. An example of this wet process is shown in Fig.5.

Time	Undercut
5 sec	120 nm
10 sec	280 nm
15 sec	450 nm
20 sec	650 nm

TABLE I. Undercut width vs. time for wet process when sample is dipped and shaken in pure DMSO solvent.

Let us now discuss some practical points related to PES :

*Humidity sensitivity* : The control of ambient humidity is crucial during the spinning of the polysulfone. The relative humidity level in a standard clean-room is about 50%. In these conditions, the visual aspect of the resist surface after spinning is grey with white points due to local phase inhomogeneity. The upper limit appears to be 25% of relative humidity during the spin coating step. A convenient solution consists of drying the atmosphere by blowing a dry nitrogen flow in a small chamber surrounding the spinner. We use a 6 dm<sup>3</sup> cylindrical plexiglass chamber which contains an hygrometer, a pipe for nitrogen flow and a small aperture on the top to inject the resist with a poly Propylene syringe onto the sample. The relative humidity is reduced to below 15% in a few minutes. Nitrogen flow was maintained during spinning. This also accelerates the evaporation of NMP solvent from the PES layer. An homogeneously colored surface is then easily obtained.

*Ageing sensitivity* : Without special storage precaution (humidity-free room), trilayers have to be used within 3 months of preparation. After this time, the PES layer could not be undercut in the specific solvent given below.

*HydroFluoric acid sensitivity* : PES polymer shows an excellent stability against HydroFluoric acid (HF) rinsing. It allows preparation of the substrate silicon surface through the mask before the metallic evaporation. HF rinsing was used in order to remove native silicon oxide. It ensures a high-quality deposited metal as it decreases hydrocarbon contaminants and passivates chemically the silicon surface. The major result was an excellent sticking of the thin lithographic structures after the final lift-off step. The surface preparation consists of 1 minute shaking of the final stencil mask in a solution of 10% in volume of HF and a 10 minutes rinsing in desionised water to remove completely the acid.

## V. TEST DEVICE

Various niobium devices have been fabricated using the above described process. The niobium was evaporated at room temperature from an electron beam gun in a ultra high vacuum chamber. No deformation of the silicon mask was observed after the electron beam evaporation. The stencil mask was lifted-off in NMP at 80°C for 10 mins followed by a few seconds in low power ultrasound (NEY ultrasonik 300). We measured the resistance of all these niobium structures using four-probes measurement with standard lock-in techniques at low temperature.

To validate the recipe, thin niobium wires were realised. We first designed the mask implementing a dry etching step in the process as described above. The geometry was a single metallic line of 5 μm long, 0.3 μm wide and 60 nm thick. The critical superconducting tem-

perature obtained was 7.2 K (see first line of Table II). Another mask using wet etching step for fabrication was tested. The structure was an array (size  $10 \mu\text{m} \times 5 \mu\text{m}$ , step  $1 \mu\text{m}$ ) of  $0.15 \mu\text{m}$  wide lines. 60 nm thick niobium were evaporated through this stencil mask. The critical temperature obtained was 7.1 K with a residual resistivity ratio (RRR) of 1.6. The same array with  $0.35 \mu\text{m}$  wide lines exhibit a  $T_c$  of 8.1 K (see line 2 and 3 in Table II). These results may be compared to a measurement on a reference plain niobium film of same thickness. In such a case,  $T_c$  is about 8K with a RRR of 1.86.

Process	RRR	w ( $\mu\text{m}$ )	e (nm)	$T_c$ (K)
dry		0.3	60	7.2
wet	1.6	0.15	60	7.1
wet		0.35	60	8.1
reference	1.86		60	8

TABLE II. Parameters (dry or wet process, resistivity ratio, line width, thickness and critical temperature) of the niobium devices.

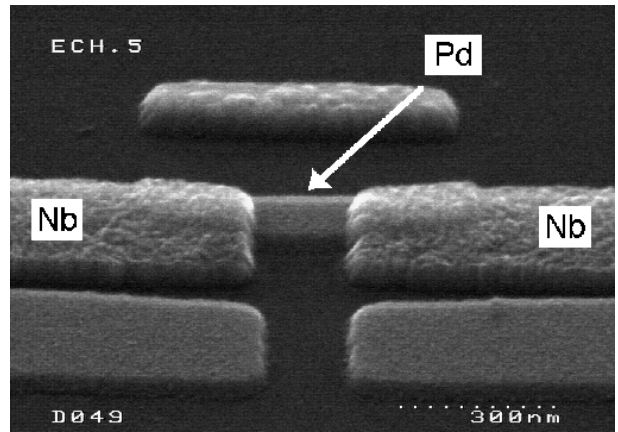


FIG. 6. Micrograph (oblique view) of a niobium-palladium-niobium SNS junction realised by shadow evaporation with high transparency S-N interfaces.

A geometry currently studied in mesoscopic physics is the superconducting - normal metal - superconducting SNS structure where the N island is viewed as a "quantum dot" coupled to superconducting electrodes through the Andreev process [14]. We are studying such SNS junctions with highly transparent interfaces [15]. The mask shown in Fig. 5 allows the in-situ fabrication of self-aligned SNS junctions by shadow evaporation using copper or palladium as the normal metal island and niobium as the superconductor. The alignment of the normal island is achieved with a nanometer scale resolution by the proper choice of the evaporation angle. High quality S-N interfaces free of contamination was ensured as the metals were evaporated within one cycle in a ultra high vacuum (UHV) chamber. A typical sample with palladium as the normal metal is shown in Fig. 6. We are making systematic measurements at low temperature of niobium-copper-niobium SNS junctions have been done. Interface resistance were estimated below  $0.2 \Omega$ . Niobium lines were  $0.3 \mu\text{m}$  wide and 60 nm thick and their resistivity was in the range of  $17\text{-}20 \mu\Omega\cdot\text{cm}$ . Copper metal was  $0.3 \mu\text{m}$  wide and 60 nm thick for a resistivity of  $4.3 \mu\Omega\cdot\text{cm}$ . In such a SNS junction the superconducting critical temperature was above 7K. Because the alignment was made in-situ under high vacuum, this technique also allows an excellent control of the interface between the central island and the external superconducting electrodes : from the metallic contact (high transparency barrier) to the weak tunnel junction (low transparency barrier). Masks with large undercuts (ses Fig. 5) can also serve to elaborate niobium based tunnel nano-junctions. Controlled oxydation of artificial or natural tunnel barriers can be performed in the UHV chamber between the two evaporations ensuring both high quality barriers and a high energy gap for niobium.

## VI. CONCLUSION

We have demonstrated a reliable technique to produce high resolution self-aligned structures by shadow evaporation of refractory metals. The key point is the use of a trilayer process with a thermostable resist bottom layer. The above recipe has been successfully tested on submicron niobium copper mesoscopic structures with excellent superconducting properties of the niobium film and excellent control of the interfaces. Using this technique we have also fabricated niobium microsquid gradiometers. This process is very promising in the area of single electronic transistors since it makes the shadow evaporation technique accessible to new materials with superior electronic properties.

## VII. ACKNOWLEDGEMENTS

We would like to acknowledge discussions with Th. Fournier, O. Buisson and H. Courtois. We would like to thank D. Mariolle and F. Martin for the S.E.M. micrographs taken at LETI-Grenoble and also D. Cousins for careful reading of the manuscript.

- [11] Wayne M Moreau, Semiconductor Lithography (Microdevices), Plenum Press, New York and London (1988)
- [12] P. J. Paniez, J. A. Guinot, B. Mortini, C. Rosilio, Microelectronic Engineering 41/42, 367-370 (1998) ; See also J. A. Guinot and P. J. Paniez, CNET DTM/MAD/97-35 internal report (1997).
- [13] In the described process, only the high resolution top resist layer is electron sensitive. The etching of the bottom layer is achieved by either wet or dry etching. However we have noticed a very small negative electron sensitivity. No specific step takes this effect into account.
- [14] See for example P. W. Brower and C. Beenakker, *Chaos and Quantum Transport in Mesoscopic Cosmos*, Chaos, Solitons and Fractals, Pergamon/Elsevier, (1997).
- [15] P. Dubos et al, to be published.

- 
- [1] For a review on single electron charging effects, see "Single Charge Tunneling, Coulomb Blockade Phenomena in nanostructures", ed. H. Grabert and M. Devoret, NATO ASI series B: Physics Vol **294** (1992), Plenum Press.
  - [2] "Mesoscopic Physics and Electronics", Nanoscience and Technology, Ed. Ando et al., Springer Verlag, Berlin Heidelberg (1998).
  - [3] P. J. Burke, R. J. Schoelkopf and D. E. Prober, J. Appl. Phys., Vol. 85, No. 3, (1999); B. Bumble and H. G. LeDuc, IEEE Transactions on Applied Superconductivity, Vol. **7**(2), (1997).
  - [4] G. J. Dolan and J. H. Dunsmuir, Physica B **152**, 7-13 (1988).
  - [5] S. P. Beaumont, P. G. Bower, T. Tamamura and C. D. W. Wilkinson, Appl. Phys. Lett. **38**, 436 (1981).
  - [6] R. E. Howard, E. L. Hu and L. D. Jackel, I.E.E.E. Transactions on Electron Devices **28**(11), 1378 (1981).
  - [7] H. Courtois, P. Gandit and B. Pannetier, Phys. Rev. B **51**, 9360 (1995).
  - [8] M. Strongin, C. Varmazis and A. Joshi, *Metallurgy of superconducting materials*, in the collection "Treatise on materials and technology" Vol. 14, ed. T. Luhman and Dew-Hughes (Academic Press, Inc. 1979), pp. 327, 347; See also J. Halbritter, Appl. Phys. A **43**, 1-28 (1987).
  - [9] H. S. J. van der Zant, H. A. Rijken and J. E. Mooij, J. Low Temp. Phys. **79**, 289 (1990).
  - [10] Y. Harada, D. B. Haviland, P. Delsing, C. D. Chen, and T. Cleason, Appl. Phys. Lett. **65**, 636 (1994).